Dynamics of dissolved oxygen isotopic ratios: a transient model to quantify primary production, community respiration, and air–water exchange in aquatic ecosystems*

Jason J. Venkiteswaran[†‡], Leonard I. Wassenaar[§], Sherry L. Schiff[†¶]

Abstract

Dissolved oxygen (O_2) is an important aquatic ecosystem health indicator. Metabolic and gas exchange rates (G), which control O_2 concentration, are affected by nutrient loading and other environmental factors. Traditionally, aquatic metabolism has been reported as primary production:community respiration (P:R) ratios using diel measurements and interpretations of dissolved O_2 and/or CO_2 concentrations, and recently using stable isotopes ($\delta^{18}O$, $\Delta^{17}O$) and steady state assumptions. Aquatic ecosystems, such as rivers and ponds, are not at steady state and exhibit diel changes, so steady state approaches are often inappropriate. A dynamic O_2 stable isotope model (photosynthesis–respiration–gas exchange; PoRGy) is presented here, requiring a minimum of parameters to quantify daily averaged P, R, and gas exchange rates under transient field conditions. Unlike steady state approaches, PoRGy can address scenarios with 100 % O_2 saturation but with $\delta^{18}O$-O_2 values that are not at air equilibrium. PoRGy successfully accounts for isotopic G when applied to an oxygen isotope equilibration laboratory experiment. PoRGy model results closely matched the diel O_2 and $\delta^{18}O$-O_2 data from three field sites with different P:R:G ratios and various P, R, and G rates. PoRGy provides a new research tool to assess ecosystem health and to pose environmental impact-driven questions. Using daily averaged rates was successful and thus they can be used to compare ecosystems across seasons and landscapes.

Introduction

Dissolved oxygen (O_2) is a crucial biogeochemical cycle in aquatic communities (Odum 1956; Stumm and Morgan 1996) because it sustains aquatic life and maintains biodiversity (Broecker 1985; Falkowski and Raven 1997). O_2 cycling is particularly sensitive to cultural eutrophication and watershed nutrient loading (Schindler 1987; Yan 2005) and is therefore a key aquatic health indicator.

Dissolved O_2 concentration is controlled to a large extent by air–water gas exchange (G) and is produced by aquatic primary production (P) and consumed by community respiration (R) at rates driven by nutrient availability, temperature, light, substrate availability, and other environmental conditions (Odum 1956; Stumm and Morgan 1996). Traditionally, aquatic metabolic status has been reported as the P:R ratio (Wilcock et al. 1998; Wetzel 2001). Ecosystem metabolic balance, whether predominantly heterotrophic (P:R < 1) or autotrophic (P:R >1), is often determined from summertime diel measurements of dissolved O_2 concentrations (Hornberger and Kelly 1975; Chapra and Di Toro 1991; Marzolf et al. 1994; Mulholland et al. 2005), by the degree O_2 or CO_2 saturation, or by light and dark bottle-incubation experiments (cf. del Giorgio and Peters 1994; Carignan et al. 2000; Prairie et al. 2002). Dissimilar aquatic ecosystems with differing P and R rates can have the same P:R ratio, casting doubt on whether the P:R ratio is a meaningful indicator of metabolic or ecological status. At the ecosystem level the chief source of error in these approaches is poor quantification of the air–water G rate. This has resulted in the development of alternative approaches to quantifying aquatic metabolism primarily by using stable oxygen isotopic ratios[1] of dissolved O_2 as tracers to constrain these three processes (P, R, G).

The study of dissolved O_2 and its ^{18}O:^{16}O (dual-isotope) isotopic ratios ($\delta^{18}O$-O_2) in various aquatic ecosystems has mainly focused on determining metabolic balance (P:R) (Quay et al. 1995; Russ et al. 2004; Parker et al. 2005) under steady state assumptions or examination of the Dole effect (Bender et al. 1994; Hoffmann et al. 2004). Recently, ^{17}O (triple-isotope) analysis has been proven useful in quantifying gross O_2 production by exploiting the ^{17}O disequilibrium between dissolved and atmospheric O_2 integrated over multi-week timescales, and in low productivity or high G environments (e.g. Luz et al. 1999; Luz and Barkan 2000; Hendricks et al. 2005, Sarma et al. 2006). The triple-isotope method has the additional advantage of avoiding the uncertainty in isotopic fractionation due to R; however, it requires laborious dual-inlet analysis (Barkan and Luz 2003), whereas dual-isotope analyses are easily automated using continuous-flow mass spectrometry, a significant cost and technical advantage where large numbers of hourly samples are required in diel studies (Wassenaar and Koehler 1999; Barth et al. 2004). Both dual- and triple-isotope approaches to date have relied on parameterised empirical models to estimate the gas exchange coefficient (k).

Almost all previously published O_2 dual- and triple-isotope studies have assumed that the aquatic ecosystem was at steady state and that neither the O_2 concentrations

*The original publication is available at www.springerlink.com in the journal Oecologia, Volume 153, Number 2, Pages 385–398, doi: 10.1007/s00442-007-0744-9.

†Department of Earth Sciences, University of Waterloo, 200 University Avenue West, Waterloo ON, N2L 3G1, Canada.

‡email: jjvenkit@uwaterloo.ca

§Environment Canada, 11 Innovation Boulevard, Saskatoon SK, S7N 3H5, Canada. Email: len.wassenaar@ec.gc.ca

¶email: sschiff@uwaterloo.ca

[1]The ^{18}O:^{16}O ratio of O_2 is measured and reported as the parts per thousand deviation from Vienna Standard Mean Ocean Water (VSMOW): $\delta = \left(\frac{R_{sample}}{R_{VSMOW}}\right)$ where R is the ^{18}O:^{16}O ratio. Isotope fractionation factors for different processes are denoted as α values: $\alpha = \frac{R_b}{R_a}$ where R is the ^{18}O:^{16}O ratio of the reactant (a) and product (b).

nor its isotopic ratios changed significantly over timeframes that ranged from hours to months (Quay et al. 1993, 1995; Wang and Veizer 2000, 2004; Russ et al. 2004; Luz and Barkan 2000; Hendricks et al. 2005; Sarma et al. 2005). This steady state assumption implies there is no significant concentration or isotopic response to a diel light cycle. While this may be valid for deep well-mixed oceanic surface studies, most natural and impacted freshwater lake and river ecosystems typically exhibit some degree of diel or seasonal productivity change. Fortunately, diel concentration and isotope dynamics can be used to better account for metabolic dynamics (e.g. Fry 2006).

Recently, Parker et al. (2005) acknowledged the problem of steady state assumptions in small rivers, but applied traditional curve analysis methods to O_2 concentration data to determine metabolic rates and k (Odum 1956). Then δ^{18}O-O_2 values were predicted using steady state equations (Quay et al. 1995) and compared to field data. Similarly (e.g. Wang and Veizer 2000; Russ et al. 2004), Parker et al. (2005) assumed an isotope fractionation factor for R. By not using a dynamic process-driven model of O_2 and its isotopes, an opportunity to use δ^{18}O-O_2 data to constrain and calculate P, R, and G, and to address the short-comings (steady state assumptions, poorly known R fractionation, poorly constrained k) was missed. The triple-isotope approach has not yet been attempted in smaller aquatic ecosystems having significant diel fluctuations.

To advance the application of O_2 isotopes in quantifying metabolic responses in freshwater ecosystems, a dynamic non-steady state O_2 concentration and δ^{18}O-O_2 (dual-isotope) model was developed. This model incorporates all of the key physical and biological processes, O_2 isotopic fractionation factors, and temporal variables (e.g. light, temperature), while using the minimum number of variables. The objectives of this paper are to: (1) describe a new dynamic O_2 and δ^{18}O-O_2 model that enables quantification of average P, R, and G rates and allows for predictive modelling; (2) illustrate the importance of quantifying both O_2 and isotopic G using experimental laboratory dissolved O_2 and δ^{18}O-O_2 data; and (3) apply the model to three aquatic ecosystems with different metabolic and G rates.

The computer model (photosynthesis–respiration–gas exchange; PoRGy) was developed to perform transient and steady state dissolved O_2 and δ^{18}O-O_2 modelling calculations and is made available to researchers at http://www.science.uwaterloo.ca/~jjvenkit/PoRGy/ or from the authors. Detailed discussion of the effect of each variable on the diel O_2 and δ^{18}O-O_2 curves and on the subsequent assessment of ecosystem health is presented elsewhere (Venkiteswaran et al. 2007).

Isotope Dynamics of *P*, *R*, and G

The O_2 generated during aquatic P is derived from oxidizing ambient water molecules. This process does not cause significant O_2 isotope fractionation (α_P = 1.000) and adds dissolved O_2 to the aquatic ecosystem with δ^{18}O values identical to that of the water (Stevens et al. 1975; Guy et al. 1989, 1993; Helman et al. 2005). The δ^{18}O-O_2 of photosynthetic O_2 added to the dissolved O_2 pool is always more depleted in ^{18}O (typically −30 to 0 ‰) than atmospheric O_2 (+23.5 ‰[2]). Given the large difference between the δ^{18}O of

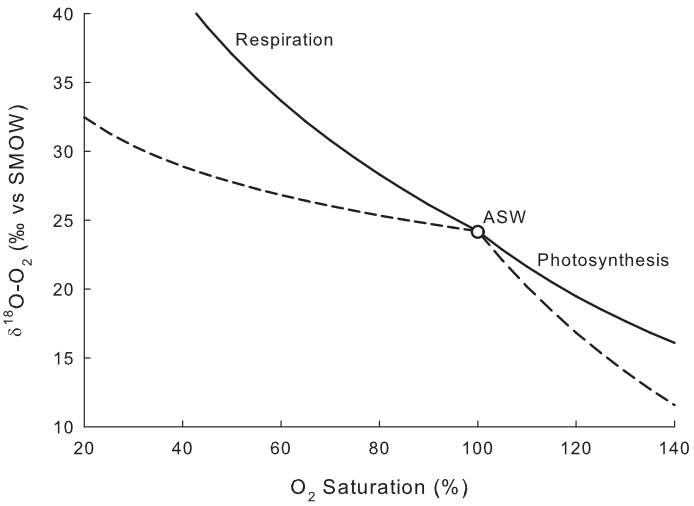

Figure 1: A graphical depiction of O_2 processes on a plot of O_2 saturation versus δ^{18}O-O_2. Respiration and photosynthesis are depicted as closed-system trajectories moving away from air-saturated water (*ASW*). The angles of the respiration and photosynthesis trajectories are controlled by α_R and δ^{18}O-H_2O respectively. Two respiration trajectories are shown, α_R=0.987 (*solid line*) and α_R=0.995 (*dashed line*), and were calculated as a unidirectional closed-system Rayleigh fractionation from ASW. Two photosynthesis trajectories are shown, δ^{18}O-H_2O=−7 ‰ (*solid line*) and δ^{18}O-H_2O=−15 ‰ (*dashed line*), and were calculated as a mixing model from ASW. Gas exchange (not shown) exhibits a curved trajectory toward ASW where an under- or super-saturated water approaches isotopic equilibrium slightly faster than approaching 100 % saturation. VSMOW Vienna standard mean oceanic water.

atmospheric O_2 and water oxygen, δ^{18}O-O_2 assays are well suited to detect the addition of small amounts of photosynthetic O_2 to aquatic ecosystems.

The rate at which aquatic photosynthetic O_2 is produced is inherently linked to incident photosynthetically active radiation (PAR). PAR increases and decreases predictably during the day (barring clouds) but in the water column can be affected by other factors (e.g. turbidity change, and variable water velocity and depth). In general, aquatic P causes daytime dissolved O_2 concentrations to increase from sunrise to shortly after solar noon and decrease thereafter. At sunset, P declines to zero and dissolved O_2 concentrations decrease due to consumption by R. A simplified depiction of the key O_2 processes (P, R, and G) versus expected δ^{18}O-O_2 values is shown in Fig. 1.

Aerobic microbial R is the principal sink for O_2 in most natural aquatic environments (Stumm and Morgan 1996; Wetzel 2001). Aquatic community R is defined as the weighted mean of all O_2 consuming pathways, which include: (1) microbial R via the cytochrome oxidase pathway in eukaryotes and the equivalent pathway in prokaryotes; (2) microbial R via the alternative oxidase pathway in eukaryotic autotrophs; (3) photorespiration in photoautotrophs (Osmond 1981); (4) the Mehler-peroxidase reaction in photoautotrophs (Laws et al. 2000); (5) chlororespiration in eukaryotes (Bennoun 2002); (6) photochemical consumption of O_2 (Miles and Brezonik 1981; Andrews et al. 2000); and (7) geochemical oxidation of reduced species such as

[2]In recent publications, atmospheric δ^{18}O-O_2 is reported to have a value of +23.8±0.3 ‰ versus VSMOW (Coplen et al. 2001), whereas others forgo conventional VSMOW-SLAP standardisation procedures and report dissolved O_2 results as ‰ deviations from local air O_2 (Luz et al. 1999).

Fe^{2+}, NH_4^+, and S. The relative importance of each pathway will likely be different for aquatic systems of differing community structure. The first two pathways are the most prevalent and occur both in light and dark, consuming organic carbon and O_2 while producing CO_2. The next two pathways only occur in the light and short-circuit photosynthetic electron transport prior to carbon fixation.

At the field scale, consumption of dissolved O_2 by the different biological pathways and aquatic organisms is combined into a single community R rate for modelling purposes. During aerobic R, the lighter O_2 isotopologue ($^{16}O^{16}O$) is preferentially consumed over the heavier O_2 isotopologue ($^{18}O^{16}O$), resulting in O_2 isotope fractionation (α_R) with the residual dissolved δ^{18}O-O_2 becoming progressively more positive. Community α_R is the weighted mean of all unique isotopic fractionation factors for each of the dissolved-O_2-consuming pathways and organisms present. The α_R values for individual species remain largely unknown; however, α_R for microbial R averages around 0.980 for a series of marine organisms, fish, and molluscs (Kiddon et al. 1993). The α_R for O_2 consumption by photorespiration and Mehler-peroxidase reactions falls between about 0.979 and 0.985 (Guy et al. 1993). Hence, at field scales α_R could range between about 0.979 and 0.985, comparable to ranges of α_R calculated from whole water closed incubations (Quay et al. 1995). However, in ecosystems where biological dissolved O_2 consumption rates are high, but where O_2 flux may be diffusion limited (e.g. within substrate), microbes become less discriminating and α_R can range from 0.994 to 1.000 (Brandes and Devol 1997; Hendry et al. 2002; Hartnett et al. 2005). Non-biological dissolved O_2 consumption may occur in aquatic systems by abiotic chemical oxygen demand (COD) as a result of discharging waste. The O_2 isotope fractionation involved in COD is likely small (cf. Taylor et al. 1984) and unknown in photochemical O_2 consumption.

Whereas P and R are unidirectional processes that either add or remove dissolved O_2 from the aquatic environment, air–water G is a bi-directional process that continuously adds and removes O_2 (and its isotopologues) from the system. The net flux of O_2 into or out of a water body can be calculated. The magnitude of the G coefficient (k) determines how quickly G occurs. Although k can be measured directly with tracer experiments, k is typically calculated using empirical models based on a few key parameters. For lakes and oceans, k is often parameterised in terms of wind speed (Gelda et al. 1996). In streams and rivers, k is often parameterized in terms of channel depth and water velocity (Moog and Jirka 1998). Despite dozens of equations that can be used to estimate k for different settings, model-calculated k values can vary by orders of magnitude for the same system (Jha et al. 2001, 2004; McBride 2002). Finally, because dissolved O_2 saturation concentrations are strongly temperature dependent (Weiss 1970), changes in water temperature will also affect the direction and rate of G. Previous O_2 dual- and triple-isotope approaches have relied on empirical models to estimate k, and this variable remains the greatest source of uncertainty (Juranek and Quay 2005).

The δ^{18}O of atmospheric O_2 is globally constant at +23.5 ‰ (Kroopnick and Craig 1972). The air–water equilibrium O_2 fractionation factor ($\alpha_{G-eq} \cong 1.0007$) (Benson et al. 1979) is the result of the small difference in solubility of each O_2 isotopologue and is not very temperature sensitive between 0 and 30 °C. Hence, dissolved O_2 in saturation equilibrium with air at Earth surface temperatures will have a δ^{18}O-O_2 of about +24.2 ‰. The kinetic O_2 fractionation factor (α_{G-k}=0.9972) is the ratio of the k of each isotopologue (Knox et al. 1992); the k for the light isotopologue is slightly larger than that of the heavy isotopologue. Even when there is no net O_2 G (i.e. at 100 % O_2 saturation), if either isotopologue is in disequilibrium, there will be a net flux of that isotopologue into or out of the aquatic ecosystem until isotopic equilibrium with air is also attained. Most studies rely on derived or empirical estimates of k; however, k can also be constrained and quantified by the shape of the diel O_2 and δ^{18}O-O_2 curves (Venkiteswaran et al. 2007).

Materials and Methods

Transient Model of Oxygen Concentration and Isotopic Ratios

To quantify the non-steady state dynamics of dissolved O_2 and δ^{18}O-O_2 in aquatic ecosystems, PoRGy was developed. PoRGy is a dynamic, process-based, computer model that combines rates of P, R, and G with their associated O_2 isotopic fractionation factors, and environmental variables such as temperature, PAR, and δ^{18}O-H_2O. The model produces transient diel curves of dissolved O_2 and δ^{18}O-O_2 that can be compared with field data. PoRGy was constructed as a box model (using Stella software, version 9.0.1, http://www.iseesystems.com/) with differential equations computed at any time interval. Thus, the effect of changing single or combined environmental parameters can be explored. PoRGy calculates the movement of the O_2 isotopologues separately, and then recombines them to produce dissolved O_2 concentrations and δ^{18}O-O_2 values for every time-step. Each of the variables is discussed below.

Photosynthesis

O_2 evolution by aquatic P is inherently related to incident light (PAR). The conventional approach to estimate P in lakes and oceans is to use a photosynthesis versus irradiance (P–E) curve. The P–E curve is modelled as a rectangular hyperbola or hyperbolic tangent curve that is linear at lower incident light and levels off at higher incident light (Falkowski and Raven 1997). Practically, the time and cost required to generate site specific P–E curves is too great to be easily applied. PoRGy instead uses theoretical daily incident light curves to adjust the rate of photosynthetic O_2 evolution. This simplification assumes that a large number of photoautotrophs are not light saturated for a significant portion of the day. This may be the case for mixed open water ecosystems, but may not be true for shallow or turbid water, or ecosystems with a large number of epiphytes or shaded submerged macrophytes. PoRGy generates daily incident light curves for any latitude, longitude, altitude, and day-of-year combination (Bird and Hulstrom 1981; van Dam 2001).

The O_2 added to the aquatic ecosystem from P has the same δ^{18}O as the water, which can be determined from a small water sample (cf. Horita and Kendall 2004). In summary, PoRGy calculates the photosynthetic addition of O_2 from a photosynthetic rate, selected by the user, modified by an incident light model (based on latitude, longitude, altitude, and date), and the measured δ^{18}O-H_2O value.

Respiration

Although the consumption of dissolved O_2 by the aquatic community combines all respiratory pathways of various organisms, the influence of α_R from each discrete pathway or group of organisms on the whole community α_R is proportional to the relative rates of O_2 consumption. The impact of fish, for example, is expected to be negligible compared to benthic microbes. PoRGy uses a single community α_R that can be adjusted or varied temporally. In shallow waters the range of α_R may be greater than in the open ocean. In previous steady state models the assumed value of a single community α_R is a limiting variable with a potentially large range (cf. Kiddon et al. 1993; Quay et al. 1995; Brandes and Devol 1997). Fortunately, the presence of a strong diel curve places constraints on α_R. The nighttime plateau (in O_2 and δ^{18}O-O_2) constrains α_R because the shapes of the diel curves approaching the plateau are different for O_2 and for δ^{18}O-O_2 and depend on α_R and k. The plateau δ^{18}O-O_2 value also depends on α_R. Thus community α_R can be determined in two ways: by best-fit modelling of the nighttime plateau and by best-fit modelling of 24-h diel data. Variance due to uncertainties in α_R is fortunately very small (Parker et al 2005; Juranek and Quay 2005; also see below).

Aquatic ecosystems may exhibit daily temperature ranges that exceed 5– 10 °C. Because the R rate increases with increasing temperature (R_T) (Kirschbaum 1995), the nominal R rate at 20 °C (R_{20}) is related to water temperature using the van 't Hoff–Arrhenius equation:

$$R_T = R_{20} \times 1.047^{T-20}$$

The temperature correction value (1.047) is a widely accepted value from water quality research and BOD_5 experiments (Bowie et al. 1985; Borsuk et al. 2004). PoRGy generates a daily water temperature regime from either a measured minimum and maximum (and related to PAR) or from a fifth-order polynomial (useful for summarising field data). In summary, PoRGy calculates O_2 consumption from a user-selected R rate, temperature regime, and α_R.

Gas Exchange

For G, four factors must to be considered: (1) the level of dissolved O_2 saturation which drives the net flux of O_2 into or out of the system; (2) the level of dissolved O_2 isotopologue saturation which drives $^{16}O^{16}O$ or $^{18}O^{16}O$ into or out of the system; (3) the air–water k; and (4) water temperature, which directly affects the previous three factors. In PoRGy, the flux of each isotopologue is modelled separately for G and is analogous to that described by Hendry et al. (2002) for soils. The $^{16}O^{16}O$ concentration can be represented by measured dissolved O_2 concentration because $^{16}O^{16}O$ comprises more than 99.75 % of the dissolved O_2. Therefore, the G equation can be written for $^{16}O^{16}O$ as:

$$G = k \times (O_{2\,\text{saturation}} - O_2)$$

where G is the net flux rate of $^{16}O^{16}O$ (O_2), O_2 is the measured dissolved O_2 concentration, and $O_{2\,\text{saturation}}$ is the temperature-dependent equilibrium saturation dissolved O_2 concentration. $O_{2\,\text{saturation}}$ is a function of temperature (Weiss 1970):

$$O_{2\,\text{saturation}} = 1.4276 \times \left[-173.4294 + 249.6339 \times \frac{100}{T} + 143.3483 \times ln\left(\frac{T}{100}\right) - 21.8392 \times \frac{T}{100} \right]$$

where $O_{2\,\text{saturation}}$ is concentration in mg L^{-1} and T is the temperature in kelvins. Diel changes in water temperature directly affect the rate and direction of G by dynamically changing the equilibrium saturation concentration.

G for the $^{18}O^{16}O$ isotopologue can be modelled using the same G equation as for total O_2 and correcting for the difference in saturation and isotope fractionation during G (Knox et al. 1992):

$$G_{^{18}O^{16}O} = k \times \alpha_{G-k} \times \left(O_{2\,\text{saturation}} \times \frac{^{18}O}{^{16}O}_{air} \times \alpha_{G-eq} - O_2 \times \frac{^{18}O}{^{16}O} \right)$$

where $G_{^{18}O^{16}O}$ is the net flux rate of $^{18}O^{16}O$ $k \times \alpha_{G-k}$ is the gas exchange coefficient for $^{18}O^{16}O$, $O_{2\,\text{saturation}} \times \frac{^{18}O}{^{16}O}_{air} \times \alpha_{G-eq}$ is the equilibrium saturation dissolved $^{18}O^{16}O$ concentration, and $O_2 \times \frac{^{18}O}{^{16}O}$ is the $^{18}O^{16}O$ concentration. In summary, PoRGy calculates G from k, O_2saturation (and therefore temperature), δ^{18}O-O_2, and appropriate fractionation factors (α_{G-k}, α_{G-eq}).

Mass Balance of *P*, *R*, and G

Arithmetically, PoRGy determines the dissolved O_2 ($^{16}O^{16}O$) concentration at any time by combining the P, R, and G equations and calculates the rate of O_2 change as:

$$\frac{dO_2}{dt} = P - R + G$$

where P, R, and G are rates as described above. PoRGy determines the $^{18}O^{16}O$ isotopologue at any time based on the ratio of isotopologues ($^{18}O^{16}O$ to $^{16}O^{16}O$) and by combining P, R, and G rates with the appropriate fractionation factors and calculates the rate of $^{18}O^{16}O$change as:

$$\frac{d^{18}O^{16}O}{dt} = P\left(\alpha_P \times \frac{^{18}O}{^{16}O}_{H_2O}\right) - R\left(\alpha_R \times \frac{^{18}O}{^{16}O}_{t}\right) + G_{^{18}O^{16}O}$$

where $\frac{^{18}O}{^{16}O}_{H_2O}$ is the isotopic ratio of H_2O.

Surface Area, and Other Model Considerations

PoRGy calculates water volume using a user-specified surface area and depth: a well-mixed, non-steady state box that is open to the atmosphere. All P, R, and G rates are calculated per unit area so all rates are directly comparable. PoRGy assumes the same water "stays in the box" during diel or temporal fluctuations, whether for ponds or rivers. In reality, few water bodies are static so the quasi steady state hydrologic assumption must be considered. For aquatic systems with a rapid flow rates or mixing (e.g. thermocline depth changes in lakes) this assumption may be valid for one or two diel cycles. However, short-term events

like diel mixing, storms, or upstream water releases from reservoirs and storm sewers may invalidate this assumption. PoRGy assumes that there are no clouds and no unexpected daytime variability in PAR or P as a result. These factors need to be taken into consideration when collecting representative field data and modelling the results.

Dissolved O_2 and δ^{18}O-O_2 field sampling for the purposes of PoRGy modelling should be made under the environmental conditions that are as typical as possible for the water body over the study period. In general, the three main factors influencing metabolic rates over diel cycles are: amount of biomass, water temperature, and light conditions. Finally, PoRGy is likely most applicable for productive water bodies (e.g. streams, rivers, and ponds) where turnover times of dissolved O_2 due to P and R are relatively rapid (hours to days) and G is lower than metabolic rates in order to produce δ^{18}O-O_2 diel patterns that can be modelled. In larger water bodies (e.g. large lakes) incomplete mixing may be a confounding factor. Nevertheless, PoRGy modelling can also be applied to ecosystems that do not exhibit diel cycles (e.g. oligotrophic systems) to obtain P, R, and G rates as long as these ecosystems are not simultaneously at 100 % O_2 saturation and isotopic equilibrium with the atmosphere.

Model Output and Sensitivity Analyses

PoRGy calculates each variable (P, R, G, dissolved O_2 concentration and saturation, δ^{18}O-O_2, temperature, and PAR) for each time-step, summarises the data, and generates two types of output: (1) tables of P, R, and G rates, dissolved O_2 concentration, saturation, and δ^{18}O-O_2 values, which can then be imported into a spreadsheet for comparison with field data; and (2) plots of the data (O_2 saturation versus δ^{18}O-O_2), which are useful for graphical comparison with field results and for comparing different model runs. Daily rates of P, R, and G can be calculated, as can the conventional P:R ratio.

Metabolic rates are unlikely to be invariant over 24 h, (even if PAR and temperature are constant). Organisms and cells grow and divide on diel time scales that exhibit circadian rhythms (cf. Falkowski and Raven 1997; Pace and Prairie 2005). Other environmental conditions may change as a result of biological, chemical, or physical activity (nutrient availability, flow rates, cloudiness, etc.). Model results from PoRGy represent a daily average that would not be expected to exactly fit each point of field data.

Results from PoRGy depend on the quality and accuracy of input parameters and assumptions. PoRGy results cannot be directly validated because it is impossible to independently and simultaneously determine all of the variables of interest in a natural system at hourly time frames (cf. Oreskes et al. 1994b), nor can the three key parameters of P, R, and α_R be measured simultaneously in the same aquatic system. Most often, P and R rates can only be obtained through incubations in bottles or submerged chambers with their associated artefacts. When there is no P at night, the cumulative effect of R and G rates and α_R may be measured simultaneously, but may not be the same as in the day. G is the only rate that can be measured independently by measuring k with another gas in a whole ecosystem tracer addition experiment. For this reason a sensitivity analysis can be used to assess the extent to which small changes in input parameters generate important changes in model results (O_2 saturation and δ^{18}O-O_2).

To assess the fit between the model-generated results and field data, two approaches were used: (1) coefficient of determination (r^2) between the PoRGy-generated dissolved O_2 and δ^{18}O-O_2 results and field data; and (2) visual comparison of both the shape and extremes of the field data to those generated by the model. An r^2 of about 0.9 or better is suggested for dissolved O_2 and δ^{18}O-O_2 between model and field data as providing an acceptable solution. While the best-fit to field results represents one possible solution for aquatic metabolism, caveats regarding the acceptance and reliability of modelling efforts apply (Konikow and Bredehoeft 1992; Oreskes et al. 1994a).

Since modelling cannot exactly replicate nature, what scientific or resource management benefits can be derived from the simplifications required by a broadly applicable model limited to key input variables? The benefits are the ability to: (1) generate average metabolic rates for the whole ecosystem (bottle incubation rates may be impractical, only short term, or limited to a subset of the ecosystem); (2) assess the influence of small or large environmental changes (akin to a sensitivity analysis); (3) test the simplifying assumptions made in the model; and (4) examine "what if" scenarios in a predictive mode. Although determining daily average P, R, and G rates is a useful objective in itself, a potential application is to quantify the effect of key metabolic and physical variables on the shape and magnitude of the diel curves in response to imposed ecological or multiple stressors (e.g. change in nutrient loading, water level, climate).

Results and Discussion

Dynamic Modelling of Isotope Gas Exchange

To assess whether PoRGy could successfully capture the dynamics of O_2 isotopic exchange when O_2 is at saturation, PoRGy was applied to the data of Knox et al. (1992). The laboratory experiment involved measurement of O_2 and δ^{18}O-O_2 for G. In the experiment, a 4 L flask of degassed water was connected to a 12 L ballast via a manometer. Pure O_2 was introduced as headspace into the smaller flask. The water was stirred slowly to minimize disturbance of the water surface. The net G rate was measured as the change in water level in the manometer. Headspace samples were analysed for δ^{18}O-O_2. Initially, the δ^{18}O-O_2 of the headspace increased because the dissolution rate of $^{16}O^{16}O$ was greater than that of $^{18}O^{16}O$ (a result of kinetic isotopic fractionation). After the water reached about 50 % saturation the δ^{18}O-O_2 of the headspace began to decline. As 100 % saturation was approached, the δ^{18}O-O_2 of the headspace continued to decline below its initial value, because of equilibrium isotopic fractionation, and the δ^{18}O of the dissolved O_2 must be greater than the δ^{18}O-O_2 of the headspace (set by the equilibrium isotopic fraction factor). Thus isotopic exchange occurs until both O_2 concentration and isotopic equilibrium are reached. The experimental data and PoRGy results are shown in Fig. 2 . The maximum and minimum δ^{18}O-O_2 values of the headspace are a function of the volumes of the headspace and water. The goodness-of-fit yielded an r^2 of 0.94 for δ^{18}O-O_2. Most importantly, PoRGy reproduced the initial increase and subsequent decrease in

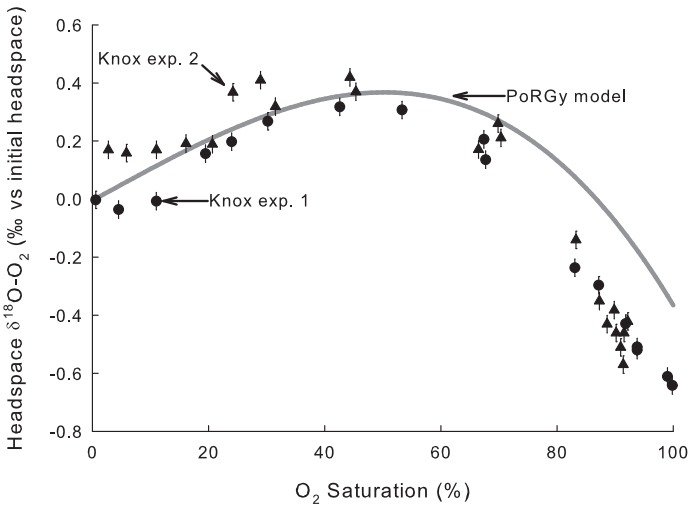

Figure 2: Comparison of the Knox et al. (1992) kinetic isotopic fractionation factor laboratory experiments (*exp.*) *(black dots and triangles)* and photosynthesis–respiration–gas exchange (*PoRGy*) (*grey line*). Axes are the same as those used by Knox et al. (1992) where the *x*-axis is the level of O_2 saturation in the water and the *y*-axis is the δ^{18}O-O_2 of the headspace versus the isotopic ratio of the initial headspace gas and not versus VSMOW. The δ^{18}O-O_2 error bars are $\pm$0.03 ‰ as reported by Knox et al. (1992).

headspace δ^{18}O-O_2 as isotopic equilibrium was dynamically established.

Steady state models used previously (Quay et al. 1995; Wang and Veizer 2000) did not allow for diel changes in O_2 or δ^{18}O-O_2 because at steady state the *P*:*R* ratio is independent of *k*. The steady state assumption is especially problematic when O_2 is at 100 % saturation but δ^{18}O-O_2 is not at equilibrium because the steady state equation is indeterminate despite the fact that *G* (to establish isotopic equilibrium) still occurs. Given that *G* remains the most problematic and primary source of error for dual- and triple-isotope assessments of aquatic metabolism (Juranek and Quay 2005), PoRGy applied to diel curves provides an improved approach. PoRGy can model isotopic *G* that was ignored in steady state approaches or assumed to occur only when O_2 saturation is not 100 %.

Dynamic modelling of field data for ecological assessment

PoRGy is applied to the field data of three sites to illustrate the potential to derive ecological information. The first example is a diel sampling of an experimental reservoir in northwestern Ontario. The Flooded Upland Dynamics Experiment (FLUDEX) was conducted at the Experimental Lakes Area (49°40′ N 93°45′ W) to study the effects of reservoir creation on greenhouse gas cycling in boreal reservoirs (cf. Bodaly et al. 2004). The Medium C reservoir was constructed by enclosing about 0.5 ha of upland forest in wooden dykes and gravel walls to a mean water depth of 0.9 m. Water was continuously pumped into the reservoir (water renewal time of 7.4 d in 2003) and the inflow and outflow monitored. In mid-July 2003, the fifth year of flooding, a 2-day diel sampling of O_2 concentration and δ^{18}O-O_2 was performed. Sunrise and sunset occurred at 0530 hours and 2110 hours (local time). Samples were collected from the outflow of the well-mixed reservoir hourly for Winkler O_2 concentration and δ^{18}O-O_2, and at 5-min intervals for O_2 saturation and temperature by a Hydrolab sonde deployed 30 cm below the surface of the water. To determine *k* directly, SF_6 was added to the reservoir and the decline in SF_6 concentration was monitored. PoRGy was run by using the independently determined *k* (0.524 cm hr^{-1}; corrected from SF_6 to O_2), a measured δ^{18}O-H_2O of -6.8 ‰, measured temperature, and latitude, longitude, and altitude. The field data and PoRGy results are shown in Fig. 3. The reservoir exhibited a strong diel cycle in both O_2 saturation and δ^{18}O-O_2 that is adequately captured with three average rates: *P*, *R*, G. The goodness-of-fit between PoRGy and the field data yielded an r^2 of 0.96 for O_2 saturation and an r^2 of 0.87 for δ^{18}O-O_2, with daily average rates of *P* and *R* of 131 and 168 mg m^{-2} hr^{-1} respectively. The gross *G* rate (sum of influx and efflux, not their difference) was 14 mg m^{-2} hr^{-1}. The diel results yielded a *P*:*R* ratio of 0.78:1 and a *P*:*R*:*G* ratio of 9.28:11.9:1. PoRGy was able to successfully reproduce both the O_2 and δ^{18}O-O_2 curves even though the system was evolving with time (i.e. mean O_2 saturation decreasing and mean δ^{18}O-O_2 increasing over two days). The reservoir was consistently well below O_2 saturation (55–85 %) with *P* < *R* and a low *k*. However, the δ^{18}O-O_2 was mostly below atmospheric equilibrium because of the large difference between δ^{18}O-H_2O, which yields O_2 for photosynthesis, and δ^{18}O of atmospheric O_2.

The second example is a diel sampling of a productive closed basin prairie slough (wetland 50) in the St. Denis National Wildlife Area east of Saskatoon (Woo and Roswell 1993). Mean water depth over the sampling period (late September 2000) was 0.165 m. Sunrise and sunset occurred at 0700 hours and 1850 hours (local time). A Hydrolab sonde recorded O_2 saturation and temperature at 15-min intervals. The sonde was placed mid-depth below the water surface at the centre of the pond. The δ^{18}O-O_2 samples were taken at 60- to 120-min intervals adjacent to the sonde, with sampling frequency increased around sunrise and sunset. To estimate *k*, wind speed was measured using the on-site meteorological station and used in common empirical models for sites with low wind speed (Crusius and Wanninkhof 2003) yielding a range of 0.93–1.24 cm hr^{-1} for *k* for O_2. PoRGy was run by using this range of *k*, an δ^{18}O-H_2O of 0 ‰ calculated from seasonal changes in δ^{18}O-H_2O from 2000 (Environment Canada, unpublished data), measured temperature, and known latitude, longitude and altitude. The field data and PoRGy results are shown in Fig. 4. The goodness-of-fit yielded an r^2 of 0.96 for O_2 saturation and an r^2 of 0.93 for δ^{18}O-O_2, with daily average rates of *P* and *R* of 105 and 143 mg m^{-2} hr^{-1} respectively. The gross *G* rate was 41 mg m^{-2} hr^{-1}. The diel results yielded a *P*:*R* ratio of 0.73:1 and a *P*:*R*:*G* ratio of 2.5:3.5:1. This productive slough exhibited a large diel change in O_2 saturation from 120 % during the day to 20 % at night. However, *P* < *R* and the mean O_2 saturation was <100 %.

The third example is a diel sampling of the South Saskatchewan River, approximately 50 km downstream of Saskatoon in mid-July 2004. A Hydrolab sonde was deployed mid-depth below the water surface to measure O_2 saturation and temperature at 15-min intervals. The depth of the river was 0.65 m and the average water velocity over the 24 h sampling period was 0.21 m s^{-1}. Sunrise and sunset occurred at 0500 hours and 2120 hours (local time). Hourly δ^{18}O-O_2 samples were collected adjacent to the sonde. To

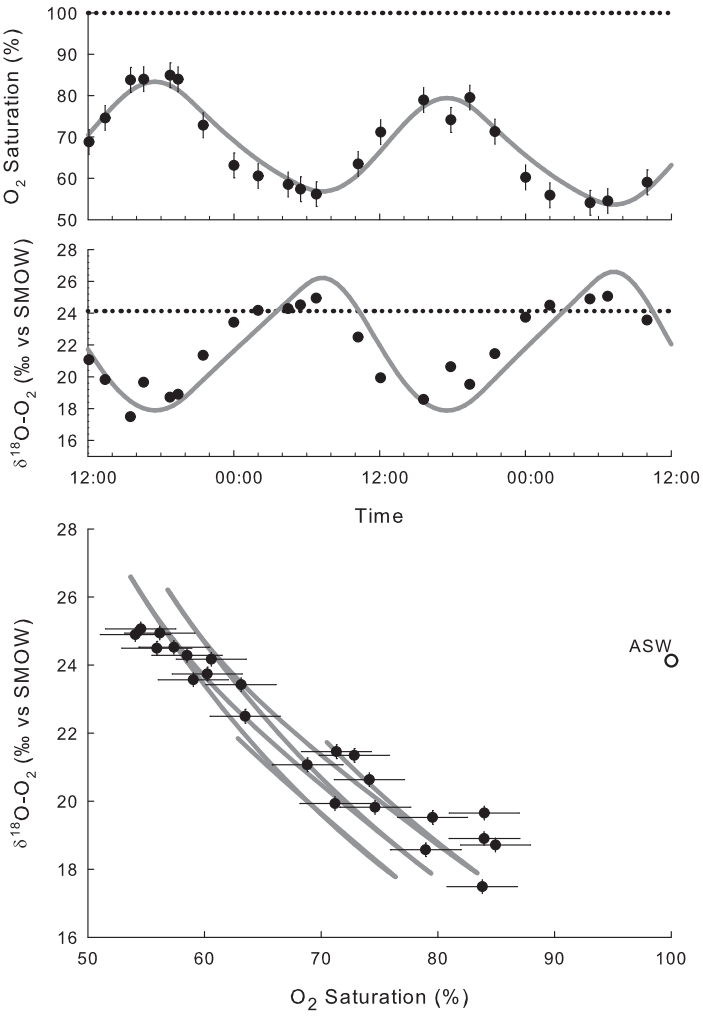

Figure 3: Field data (*black dots*) with 1 SD error bars (±0.2 % and ±0.2 ‰) and PoRGy model (*grey line*) diel data from the Flooded Upland Dynamics Experiment Medium C reservoir from 23 to 25 July 2003. The frequency of O_2 saturation data is reduced to match the δ^{18}O-O_2 data. Equilibrium saturation is shown as dotted lines in the temporal figures and ASW is shown in the cross-plot. For abbreviations, see Figs. 1 and 2.

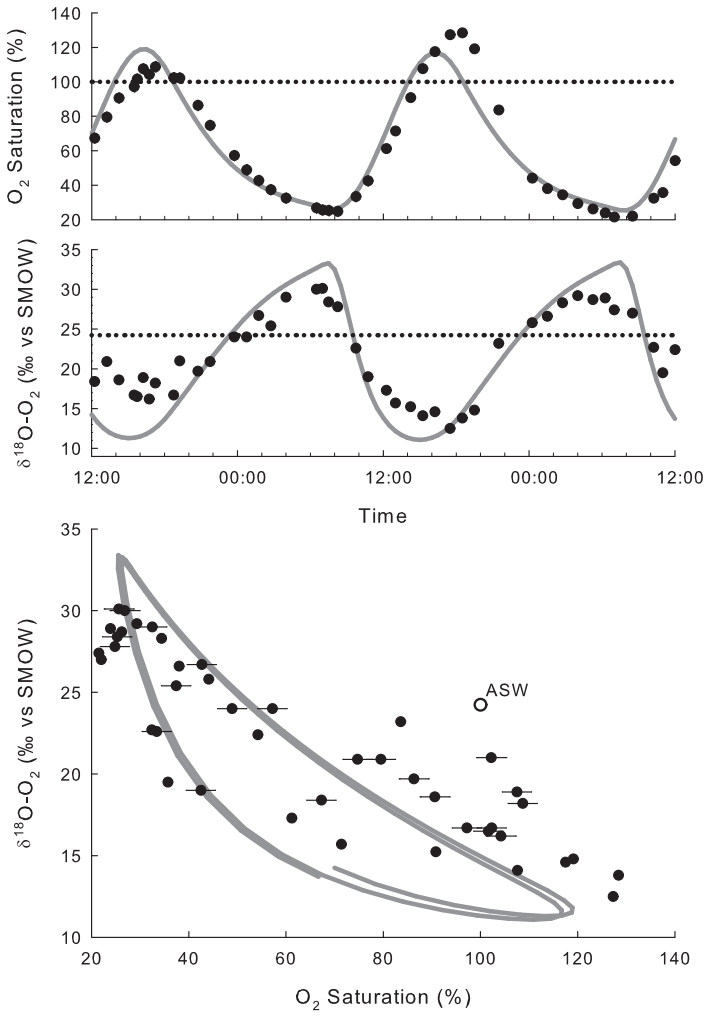

Figure 4: Field data (*black dots*) with 1 SD error bars (±0.2 % and ±0.2 ‰) and PoRGy model (*grey line*) diel data from the pond 50 in St. Denis National Wildlife Area from 28 to 29 July 2000. The frequency of O_2 saturation data is reduced to match the δ^{18}O-O_2 data. Equilibrium saturation is shown as dotted lines in the temporal figures and ASW is shown in the cross-plot. For abbreviations, see Figs. 1 and 2.

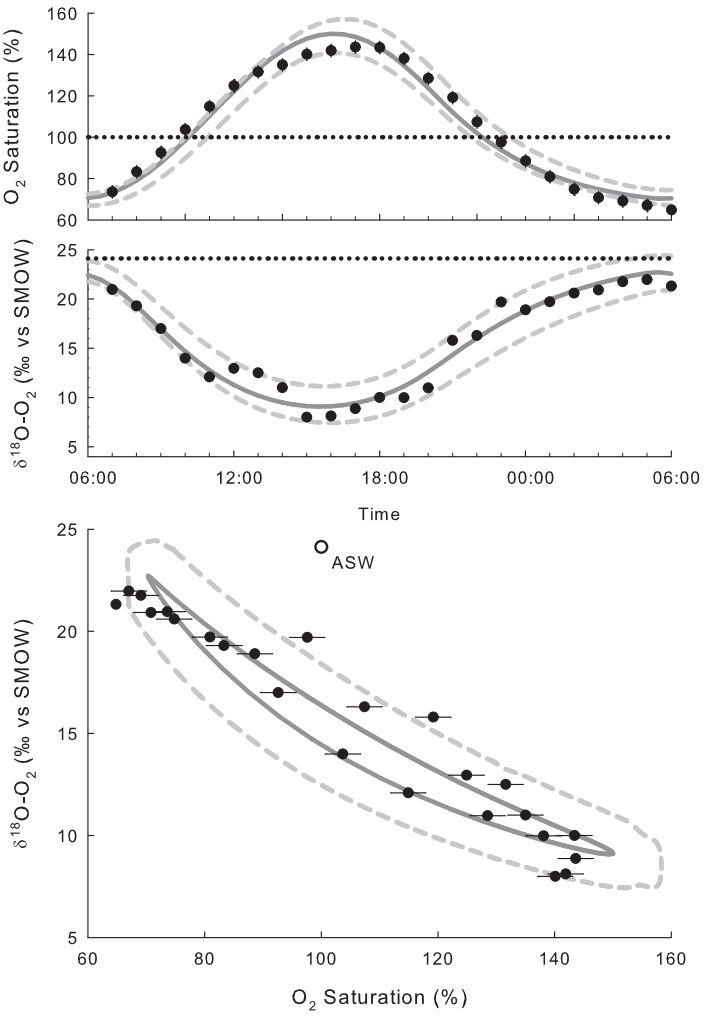

Figure 5: Field data (*black dots*) with 1 SD error bars (±0.2 % and ±0.2 ‰) and PoRGy model (*grey line*) diel data from the South Saskatchewan River near Saskatoon from from 14 to 15 July 2004 . The frequency of O_2 saturation data is reduced to match the δ^{18}O-O_2 data. Equilibrium saturation is shown as dotted lines in the temporal figures and air-saturated water (ASW) is shown in the cross-plot. The "sensitivity cloud" (*light grey dashed line*) around the best-fit was created based on ±5 % of the metabolic rates, ±10 % of gas exchange coefficient, ±0.003 of α_R, and ±0.3 of δ^{18}O-H_2O. For abbreviations, see Figs. 1 and 2.

estimate k, depth and velocity measurements were used in four common river empirical models (O'Connor and Dobbins 1958; Churchill et al. 1962; Owens et al. 1964; Langbein and Durum 1967) yielding a range in k of 4.2 to 7.1 cm hr^{-1}. PoRGy was run by allowing k to fluctuate within this range, a measured δ^{18}O-H_2O of –7 ‰, measured temperature, and known latitude, longitude, and altitude. The field data and PoRGy results are shown in Fig. 5. The goodness-of-fit yielded an r^2 of 0.98 for O_2 saturation and an r^2 of 0.97 for δ^{18}O-O_2, with daily average rates of P and R of 425 and 382 mg m^{-2} hr^{-1} respectively. The gross G rate was 215 mg m^{-2} hr^{-1}. The diel results yielded a P:R ratio of 1.11:1 and a P:R:G ratio of 1.97:1.78:1. The river had a large diel in both O_2 saturation and δ^{18}O-O_2. The mean O_2 saturation exceeded 100 % because $P > R$ but the δ^{18}O-O_2 was consistently below atmospheric equilibrium because of the high P rate adding O_2 with the δ^{18}O-H_2O of -7 ‰.

The sensitivity of model results to the input parameters can be easily assessed with PoRGy. A reasonable range for each unknown input parameter can be used and the resulting curves plotted together generating a "sensitivity cloud" or "error space" around the field data. A range of ±5 % in metabolic rates is comparable to the measured error in typically laboratory incubations. A range of ±10 % in k is representative of the variability in k estimated by empirical wind speed equations or depth and velocity equations (cf. Crusius and Wanninkhof 2003; Jha et al. 2001). A range of ±0.003 in α_R is typical of laboratory incubations (e.g. Kiddon et al. 1993; Quay et al. 1995). A range of ±0.3 ‰ in δ^{18}O-H_2O is comparable to the largest error expected among the commonly used analytical methods summarised by Horita and Kendall (2004). A matrix of all possible combinations of the above ranges in P, R, k, α_R, and δ^{18}O-H_2O were modelled using PoRGy for the South Saskatchewan River example and presented as the "sensitivity cloud" circumscribing the field data and best-fit results in Fig. 5. The best-fit results of the South Saskatchewan River involved finding P and R rates, a k value within a specified range, and an α_R value that minimised the difference between model output and field data. Thus any changes in those parameters to create the "cloud" necessarily reduced the goodness-of-fit. Thus the P and R rates, and k and α_R values are together best-fit values (Table 1). The r^2-values of the generated diel curves contained within the cloud ranged from 0.96 to 0.98. The sensitivity of model output to changes in the R fractionation factor (α_R) value was low, confirming the observations of others (Juranek and Quay 2005; Parker et al. 2005). Similarly, sensitivity of model results to only one variable or a combination of two or more variables is easily assessed.

PoRGy successfully modelled diel data ($r^2 \geq 87$ %) for three field sites with a large range in P, R, and G, and differing mean O_2 saturation and mean δ^{18}O-O_2. PoRGy used daily average input parameters to generate daily average P, R, and G rates. Even though daily rates are used, the overall goodness-of-fit between model output and field data is good even in ecosystems that are evolving over the sampling period. The FLUDEX reservoir and prairie slough have similar P and R rates, P:R ratio, mean O_2 and mean δ^{18}O-O_2. The prairie slough has a much larger diel range in O_2 (20–120 %) and δ^{18}O-O_2 (12–30 ‰) than the FLUDEX reservoir. However, k is much higher in the sough and thus the P:R:G ratio (2.5:3.5:1) is also much different than in the reservoir (9.3:11.9:1). Thus the relative magnitude of P and R cannot be immediately assessed by simply comparing diel curves. O_2 diel curves (and δ^{18}O-O_2 curves) exhibit the balance between P, R, and G. The South Saskatchewan River has much higher P and R rates than either the slough or reservoir. The magnitude of the diel range, however, is less than the slough due to the much higher G. Ecosystems can be compared with P and R rates or P:R:G ratios; both offer more detail that the P:R ratio. In P:R ratio studies, G is often not determined directly. PoRGy facilitates the comparison by calculating average P, R, and G rates, and thus the P:R:G ratio, over the diel cycle.

Some parameters used to model the field examples were assumed to be fixed or a daily average (e.g. k, flow rates, α_R) although some of these may have changed on hourly timescales. Practically, instantaneous rates are of little broad interest, hence an absolute model fit to field data was neither expected nor required. Nevertheless, the results show that large diel changes are more apparent and easily mea-

Table 1: PoRGy model input parameters and results for examples shown in Figs. **??**, **??**, and **??**. *FLUDEX* Flooded Upland Dynamics Experiment, P primary production, R community respiration, G gas exchange, k G coefficient, G^* gross G (sum of influx and efflux, not their difference)

Example	Input variables: Independently known	Input variables: Adjusted to improve fit (rates are mg m^{-2} hr^{-1})	Calculated from model fit (rates are mg m^{-2} hr^{-1})
FLUDEX Medium C reservoir, Experimental Lakes Area, northwestern, Ontario	δ^{18}O-H_2O=−6.8 ‰ latitude=49.6639° longitude=−93.7221° altitude=424 masl k=0.005 24 m hr^{-1} temperature=21–25°C depth=0.9 m area=4,900 m^2 day of year=204 year=2003	P_{max}=510 R_{20}=150 α_R=0.979	P=131 R=168 G^*=14 P:R=0.78:1 P:R:G=9.28:11.9:1
Wetland 50, St. Denis National Wildlife Area	δ^{18}O-H_2O=0 ‰ latitude=51.2167° longitude=−106.267° altitude=550 masl temperature=7–17°C depth=0.165 m area=11,040 m^2 day of year=271 year=2000	P_{max}=830 R_{20}=200 k=0.0093 m hr^{-1} α_R=0.985	P=105 R=143 G^*=41 P:R=0.73:1 P:R:G=2.5:3.5:1
South Saskatchewan River, 50 km downstream from Saskatoon	δ^{18}O-H_2O=−7 ‰ latitude=52.5104° longitude=−106.4146° altitude=550 masl temperature=20.4–24.5°C depth=0.65 m area=1 m^2 day of year=197 year=2004	P_{max}=1640 R_{20}=340 k=0.1072 m hr^{-1} α_R=0.998	P=425 R=382 G^*=215 P:R=1.11:1 P:R:G=1.97:1.78:1

surable in lower G environments like ponds compared to higher G environments like rivers (Table 1; Figures 3, 4, and 5) since the latter require relatively higher metabolic rates to maintain diel changes in O_2 and $\delta^{18}O$-O_2.

Dynamic modelling with PoRGy has captured the main features of the diel O_2 and $\delta^{18}O$-O_2 curves: the timings and values of the maxima and minima. The simplifications in PoRGy such as using average values, even though ecosystems do not operate with average values, did not hinder the best-fit modelling. An important benefit derived from average P, R, and G rates is the ability to compare ecosystems seasonally, longitudinally, and with each other. Comparing the three field examples shows that ecosystems can have large diel ranges in O_2 and $\delta^{18}O$-O_2 with widely different P:R:G ratios and rates and thus different ecosystem functions.

Conclusion

Most aquatic systems of interest, and especially human-impacted systems, are not at steady state and exhibit significant diel O_2 cycles. Transient modelling is therefore required if reasonable estimates of P:R:G ratios and P, R, and G rates are needed to quantify the cumulative impact of anthropogenic stressors on community metabolism. The transient model (PoRGy) approach solves dynamic O_2 and $\delta^{18}O$-O_2 mass balances using a minimum number of key variables. The model generates dissolved O_2 concentration and $\delta^{18}O$-O_2 diel curves that can be compared to field data. By changing rates of biological processes (P and R), G, the O_2 isotopic fractionation factors, light curves, and temperature, each of the key variables may be further examined for its role and relative importance in the shape of the hysteretic diel curve. PoRGy allows researchers to quickly visualise the sensitivity of small changes in the environmental variables to the overall rates and metabolic balance in aquatic systems.

The PoRGy model provides daily fundamental ecological rates. Users can employ PoRGy to pose impact- and process-driven causal environmental questions, such as: how does a nutrient-driven 5 % increase in metabolic rates affect O_2 status under the same G regime? Or, how does a 2 °C increase in water temperature affect R outcomes? Periodic diel $\delta^{18}O$-O_2 surveys in conjunction with basic O_2 saturation data can provide river managers with both metabolic rates and a method for deriving G rates necessary for watershed models.

Acknowledgements

This work was supported by a Natural Sciences and Engineering Research Council of Canada (NSERC) Strategic grant (S. L. S. and L. I. W.), Environment Canada (L. I. W.), the Canadian Foundation for Climate and Atmospheric Sciences (CFCAS) (S. L. S.), an Ontario Graduate Scholarship (J. J. V.), and Environment Canada's Science Horizons Youth Internship Program (S. L. S.). Analytical development at the University of Waterloo was funded by an NSERC Discovery grant (S. L. S.), CFCAS (S. L. S.), and the Centre for Research in Earth and Space Technology (S. L. S.). Andrea Wojtyniak, Kevin Maurice, and Matthijs Vlaar provided field assistance. Richard Elgood, Geoff Koehler, and Daryl Halliwell provided additional field and laboratory assistance. FLUDEX was funded by Fisheries and Oceans Canada, Manitoba Hydro, and Hydro-Québec.

References

Andrews SS, Caron S, Zafiriou OC (2000) Photochemical Oxygen Consumption in Marine Waters: A Major Sink for Colored Dissolved Organic Matter? *Limnol Oceanogr* 45:267–277

Barkan E, Luz B, (2003) Measurements of $^{17}O/^{16}O$ and $^{18}O/^{16}O$ of O_2 and O_2/Ar ratio in air. *Rapid Commun Mass Spec* 17:2809–2814. doi:10.1002/rcm.1267

Barth JAC, Tait A, Bolshaw M (2004) Automated analyses of $^{18}O/^{16}O$ ratios in dissolved oxygen from 12-mL water samples. *Limnol Oceanogr Meth* 2:35–41

Bender ML, Sowers T, Labeyrie L (1994) The Dole effect and its variations during the last 130,000 years as measured in the Vostok ice core. *Global Biogeochem Cycles* 8:363–376

Bennoun P (2002) The present model for chlororespiration. *Photosyn Res* 73:273–277

Benson BB, Krause D Jr, Peterson MA (1979) The solubility and Isotopic Fractionation of Gases in Dilute Aquatic Solution. I. Oxygen. *J Solution Chem* 8:655–690

Bird RE, Hulstrom RL (1981) A Simplified Clear Sky Model for Direct and Diffuse Insolation on Horizontal Surfaces. SERI/TR-642-761. Solar Energy Research Institute, Golden

Bodaly RA, Beaty KG, Hendzel LH, Majewski AR, Paterson MJ, Rolfhus KR, Penn AF, St.Louis VL, Hall BD, Matthews CJD, Cherewyk KA, Mailman M, Hurley JP, Schiff SL, Venkiteswaran JJ (2004) The use of experimental reservoirs to explore the mercury and greenhouse gas impacts of hydro-electric developments: The FLUDEX experiment. *Environ Sci Technol* 38:337A–352A

Borsuk ME, Stow CA, Reckhow KH (2004) Confounding Effect of Flow on Estuarine Response to Nitrogen Loading. *J Environ Eng ASCE* 130:605–614. doi:10.1061/(ASCE)0733-9372(2004)130:6(605)

Bowie GL, Mills WB, Porcella DB, Campbell CL, Pagenkopf JR, Rupp GL, Johnson KM, Chan PWH, Gherini SA, Chamberlin CE (1985) Rates, constants, and kinetic formulations in surface water quality modelling, 2nd edn. EPA/600/3-85/040, USEPA, Athens

Brandes JA, Devol AH (1997) Isotopic fractionation of oxygen and nitrogen in coastal marine sediments. *Geochim Cosmochim Acta* 61:1793–1801

Broecker WS (1985) How to build a habitable planet. Eldigio Press, Palisades

Chapra SC, Di Toro DM (1991) Delta Method for Estimating Primary Production, Respiration, and Reaeration in Streams. *J Environ Eng ASCE* 117:640–655

Carignan R, Planas D, Vis C (2000) Planktonic production and respiration in oligotrophic Shield lakes. *Limnol Oceanogr* 45:189–199

Churchill MA, Elmore HL, Buckingham RA (1962) The prediction of stream reaeration rates. *J Environ Eng ASCE* 88(SA4):1–46

Coplen TB, Hopple JA, Böhlke JK, Peiser HS, Rieder SE, Krouse HR, Rosman KJR, Ding T, Vocke Jr. RD, Révész KM, Lamberty A, Taylor P, De Bièvre P (2001) Compilation of minimum and maximum isotope ratios of selected elements in naturally occurring terrestrial materials and reagents. US Geological Survey Water-Resources Investigations Report 01-4222. USGS.

Crusius J, Wanninkhof R (2003) Gas transfer velocities measured at low wind speed over a lake. *Limnol Oceanogr* 48:101–1017

del Giorgio PA, Peters DH (1994) Patterns in planktonic P : R ratios in lakes: Influence of lake trophy and dissolved organic carbon. *Limnol Oceanogr* 39:772–787

Falkowski PG, Raven JA (1997) Aquatic photosynthesis. Blackwell, Malden

Fry, B (2006) Stable Isotope Ecology. Springer, Berlin Heidelberg New York

Gelda RK, Auer MT, Effler SW, Chapra SC, Storey ML (1996) Determination of reaeration coefficients: Whole-lake approach. *J Environ Eng ASCE* 122:269–275. doi:10.1061/(ASCE)0733-9372(1996)122:4(269)

Guy RD, Berry JA, Fogel ML, Hoering TC (1989) Differential Fractionation of Oxygen Isotopes by Cyanide-Resistant and Cyanide-Sensitive Respiration in Plants. *Planta* 177:483–491

Guy RD, Fogel ML, Berry JA (1993) Photosynthetic fractionation of the stable isotopes of oxygen and carbon. *Plant Physiol* 101:37–47

Hartnett H, Devol A, Brandes J, Chang B (2005) Oxygen isotope fractionation in marine sediments during respiration. *Geochim Cosmochim Acta* 69:A579

Helman Y, Barkan E, Eisenstadt D, Luz B, Kaplan A (2005) Fractionation of the three stable oxygen isotopes by oxygen-producing and oxygen-consuming reactions in photosynthetic organisms. *Plant Physiol* 138:2292–2298. doi:10.1104/pp.105.063768

Hendricks MB, Bender ML, Barnett BA, Strutton P, Chavez FP (2005) Triple isotope composition of dissolved O_2 in the equatorial Pacific: A tracer

of mixing, production, and respiration. *J Geophys Res* 110:C12021 doi:10.1029/2004JC002735

Hendry MJ, Wassenaar LI, Birkham TK (2002) Microbial respiration and diffusive transport of O_2, $^{16}O_2$, and $^{18}O^{16}O$ in unsaturated soils: A mesocosm experiment. *Geochim Cosmochim Acta* 66:3367–3374 doi:10.1016/S0016-7037(02)00949-3

Hoffmann G, Cuntz M, Weber C, Ciais P, Friedlingstein P, Heinmann M, Jouzel J, Kaduk J, Maier-Reimer E, Seibt U, Six K (2004) A model of the Earth's Dole effect. *Global Biogeochem Cycles* 18:GB1008 doi:10.1029/2003GB002059

Horita J, Kendall C (2004) Stable isotope analysis of water and aqueous solutions by conventional dual-inlet mass spectrometry. In: de Groot PA (ed) Handbook of Stable Isotope Analytical Techniques, vol 1. Elsevier, Amsterdam, pp 1–37

Hornberger GM, Kelly MG (1975) Atmospheric Reaeration in a River Using Productivity Analysis. *J Environ Eng ASCE* 101:729–739

Jha R, Ojha CSP, Bhatia KSS (2001) Refinement of predictive reaeration equations for a typical Indian river. *Hydrol Proc* 15:1047–1060 doi:10.1002/hyp.177

Jha R, Ojha CSP, Bhatia KSS (2004) A supplementary approach for estimating reaeration rate coefficients. *Hydrol Proc* 18:65–79 doi:10.1002/hyp.1312

Juranek LW, Quay PD (2005) In vitro and in situ gross primary and net community production in the North Pacific Subtropical Gyre using labelled and natural abundance isotopes of dissolved O_2. *Global Bioeochemical Cycles* 19:GB3009. doi:10.1029/2004GB002384

Kiddon J, BenderML, Orchardo J, Caron DA, Goldman JC, Dennett M (1993) Isotopic Fractionation of Oxygen by Respiring Marine Organisms. *Global Biogeochem Cycles* 7:679–694

Kirschbaum MUF (1995) The Temperature-Dependence of Soil Organic-Matter Decomposition, and the Effect of Global Warming on Soil Organic-C Storage. *Soil Biol. Biochem.* 27:753–760

Knox M, Quay PD, Wilbur D (1992) Kinetic Isotopic Fractionation During Air–Water Gas Transfer of O_2, N_2, CH_4, and H_2. *J Geophys Res* 97:20335–20343

Konikow LF, Bredehoeft JD (1992) Groundwater Models Cannot Be Validated. *Adv Wat Res* 15:75–83

Kroopnick P, Craig H (1972) Atmospheric oxygen: Isotopic composition and solubility fractionation. *Science* 175:54–55

Langbein WB, Durum WH (1967) The Aeration Capacity of Streams. USGS Circular No. 542. USGS, Washington, D.C.

Laws EA, Landry MR, Barber RT, Campbell L, Dickson M-L, Marra J (2000) Carbon cycling in primary production bottle incubations: inferences from grazing experiments and photosynthetic studies using ^{14}C and ^{18}O in the Arabian Sea. *Deep-Sea Res. II* 47:1339–1352. doi:10.1016/S0967-0645(99)00146-0

Luz B, Barkan E (2000) Productivity with the Triple-Isotope Composition of Dissolved Oxygen. *Science* 288:2028–2031

Luz B, Barkan E, Bender ML, Thiemens MH, Boering KA (1999) Triple-isotope composition of atmospheric oxygen as a tracer of biosphere productivity. *Nature* 400:547–550. doi:10.1038/22987

Marzolf ER, Mulholland PJ, Steinman AD (1994) Improvements to the Diurnal Upstream–Downstream Dissolved-Oxygen Change Technique for Determining Whole-Stream Metabolism in Small Streams. *Can J Fish Aquat Sci* 51:1591–1599

McBride GB (2002) Calculating stream reaeration coefficients from oxygen profiles. *J Environ Eng ASCE* 128:384–386. doi:10.1061/(ASCE)0733-9372(2002)128:4(384)

Miles CJ, Brezonik PL (1981) Oxygen consumption in humic-colored waters by a photochemical ferrous-ferric catalytic cycle. *Environ Sci Technol* 15:1089–1095. doi:10.1021/es00091a010

Moog DB, Jirka GH (1998) Analysis of reaeration equations using mean multiplicative error. *J Environ Eng ASCE* 124:104–110. doi:10.1061/(ASCE)0733-9372(1998)124:2(104)

Mulholland PJ, Houser JN, Maloney KO (2005) Stream diurnal dissolved oxygen profiles as indicators of in-stream metabolism and disturbance effects: Fort Benning as a case study. *Ecol Indicat* 5:243–252. doi:10.1016/j.ecolind.2005.03.004

O'Connor DJ, Dobbins WE (1958) Mechanism of reaeration in natural streams. *Am Soc Civ Eng Trans* 123:641–684

Odum HT (1956) Primary Production in Flowing Waters. *Limnol Oceanorg* 1: 102–117

Oreskes N, Belitz K, Shraderfrechette K (1994a) The Meaning of Models—Response. *Science* 264:331–331

Oreskes N, Shraderfrechette K, Belitz K (1994b) Verification, Validation, and Confirmation of Numerical-Models in the Earth-Sciences. *Science* 263:641–646

Osmond CB (1981) Photorespiration and Photoinhibition Some Implications for the Energetics of Photosynthesis. *Biochim Biophys Acta* 639:77–98. doi:10.1016/0304-4173(81)90006-9

Owens M, Edwards RW, Gibbs JW (1964) Some reaeration studies in streams. *Air Water Pollut.* 35:469–486

Pace ML, Prairie YT (2005) Respiration in lakes. In: del Giorgio PA, Williams PjleB (eds) Respiration in Aquatic Ecosystems. Oxford University Press, Oxford, pp 103–121

Parker SR, Poulson SR, Gammons CH, Degrandpre MD (2005) Biogeochemical controls on diel cycling of stable isotopes of dissolved O_2 and dissolved inorganic carbon in the Big Hole River, Montana. *Environ Sci Technol* 39:7134–7140 doi:10.1021/es0505595

Prairie YT, Bird DF, Cole JC (2002) The summer metabolic balance in the epilimnion of southeastern Quebec lakes. *Limnol Oceanogr* 47:316–321

Quay PD, Emerson S, Wilbur DO, Stump C (1993) The $\delta^{18}O$ of dissolved O_2 in the surface waters of the sub-arctic pacific: a tracer of biological productivity. *J Geophys Res* 98:8447–8458

Quay PD, Wilbur DO, Richey JE, Devol AH (1995) The ^{18}O:^{16}O of dissolved oxygen in rivers and the lakes in the Amazon Basin: Determining the ratio of respiration to photosynthesis rates in freshwater. *Limnol Oceanogr* 40:718–729

Russ ME, Ostrom NE, Gandhi H, Ostrom PH, Urban NR (2004) Temporal and spatial variations in R:P ratios in Lake Superior, an oligotrophic freshwater environment. *J Geophys Res* 109:C10S12 doi:10.1029/2003JC001890

Sarma VVSS, Abe O, Hashimoto S, Hinuma A, Saino T (2005) Seasonal variations in triple oxygen isotopes and gross oxygen production in the Sagami Bay, central Japan. *Limnol Oceanogr* 50:544–552

Sarma VVSS, Abe O, Hinuma A, Saino T (2006) Short-term variation of triple oxygen and gross oxygen production in the Sagami Bay, central Japan. *Limnol Oceanogr* 51:1432–1442

Schindler DW (1987) Detecting ecosystem responses to anthropogenic stress. *Can J Fish Aquat Sci* 44[Suppl 1]:6–25

Stevens CLR, Schultz D, Vanbaalen C, Parker PL (1975) Oxygen Isotope Fractionation During Photosynthesis in a Blue-Green and a Green-Alga. *Plant Physiol* 56:126–129

Stumm W, Morgan JJ (1996) Aquatic chemistry, third edn. Wiley–Interscience, New York

Taylor BE, Wheeler MC, Nordstrom DK (1984) Stable Isotope Geochemistry of Acid-Mine Drainage—Experimental Oxidation of Pyrite. *Geochim Cosmochim Acta* 48:2669–2678

van Dam, O (2001) Forest filled with gaps. Effects of gap size on water and nutrient cycling in tropical rain forest. A Study in Guyana. PhD thesis, Utrecht University, Utrecht

Venkiteswaran JJ, Schiff SL, Wassenaar LI (2007) Aquatic metabolims and ecosystem health assessment using dissolved O_2 stable isotope diel curves. *Ecol Appl* in review

Wang XF, Veizer J (2000) Respiration-photosynthesis balance of terrestrial aquatic ecosystems, Ottawa area, Canada. *Geochim Cosmochim Acta* 64:3775–3786 doi:10.1016/S0016-7037(00)00477-4

Wang XF, Veizer J (2004) Erratum to Xuefeng Wang and Jan Veizer (2000), respiration–photosynthesis balance of terrestrial aquatic ecosystems, Ottawa area, Canada. Geochim Cosmochim Acta 64(22), 3775–3786. *Geochim Cosmochim Acta* 68:933–944 doi:10.1016/S0016-7037(03)00490-3

Wassenaar LI, Koehler G (1999) An on-line technique for the determination of the $\delta^{18}O$ and $\delta^{17}O$ of gaseous and dissolved oxygen. *Anal Chem* 71:4965–4968

Weiss RF (1970) Solubility of Nitrogen, Oxygen and Argon in Water and Seawater.*Deep-Sea Res.* 17:721–735

Wetzel R (2001) Limnology—Lake and River Ecosystems. Academic Press, San Diego, Calif.

Wilcock RJ, Nagels JW, McBride GB, Collier KJ, Wilson BT, Huser BA (1998) Characterisation of lowland streams using a single-station diurnal curve analysis model with continuous monitoring data for dissolved oxygen and temperature. *N Z J Mar Fresh Res* 32:67–79

Woo M-K, Roswell R.D. (1993) Hydrology of a prairie slough. *J Hydrol* 146:175–207

Yan ND (2005) Research needs for the management of water quality issues, particularly phosphorus and oxygen concentrations, related to salmonid cage aquaculture in Canadian freshwaters. *Environ Rev* 13:1–19. doi:10.1139/A05-001